

CAUSAL VIDEO SUMMARIZER FOR VIDEO EXPLORATION

Jia-Hong Huang¹, Chao-Han Huck Yang², Pin-Yu Chen³, Andrew Brown¹, Marcel Worring¹

¹University of Amsterdam, Netherlands ²Georgia Institute of Technology, USA ³IBM Research, USA
j.huang@uva.nl, huckiyang@gatech.edu, pin-yu.chen@ibm.com, a.g.brown@uva.nl, m.worring@uva.nl

ABSTRACT

Recently, video summarization has been proposed as a method to help video exploration. However, traditional video summarization models only generate a fixed video summary which is usually independent of user-specific needs and hence limits the effectiveness of video exploration. Multi-modal video summarization is one of the approaches utilized to address this issue. Multi-modal video summarization has a video input and a text-based query input. Hence, effective modeling of the interaction between a video input and text-based query is essential to multi-modal video summarization. In this work, a new causality-based method named Causal Video Summarizer (CVS) is proposed to effectively capture the interactive information between the video and query to tackle the task of multi-modal video summarization. The proposed method consists of a probabilistic encoder and a probabilistic decoder. Based on the evaluation of the existing multi-modal video summarization dataset, experimental results show that the proposed approach is effective with the increase of +5.4% in accuracy and +4.92% increase of $F1$ -score, compared with the state-of-the-art method.

1. INTRODUCTION

Video contents are growing at an ever-increasing speed and beyond the capacity of an individual for full comprehension. According to [1], more than 18,000 hours of videos are uploaded to YouTube per minute. Exploring this quantity of video data is a daunting task, and video summarization is gaining traction as the ideal solution [2, 3]. The main idea of video summarization is to automatically generate a short video clip that summarizes the content of an original, longer video by capturing its important parts [4–6]. However, traditional video summarization approaches, e.g., [7, 8], only create a fixed video summary for a given video. Given that viewers may have different preferences and videos have different ideal summarization, this issue reduces the effectiveness of video exploration.

Multi-modal video summarization has been proposed as an approach to improve the effectiveness of video exploration [9, 10]. It generates video summaries for a given video based on the text-based query provided by the user, illustrated in Figure 1. Conventional video summarization only has video input modality, while an efficient choice for multi-modal video summarization is a text-based query, in addition to video [9, 10]. When multi-modal video summarization is used to help video exploration, effectively modeling the implicit relation/interaction between the text-based query and

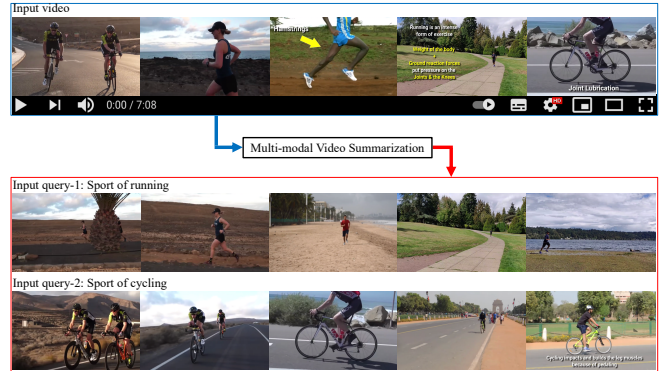


Fig. 1: Multi-modal video summarization. The input video is summarised taking into account text-based queries. “Input query-1: Sport of running” and “Input query-2: Sport of cycling” independently drive the model to generate video summaries that contain running-related content and cycling-related content, respectively.

the video is important [9]. In [10], the proposed model exploits a joint representation of vision and language to perform multi-modal video summarization. However, the implicit interaction between the query and the video is not properly modeled because the simple average-based method used in [10] probably is not effective enough.

As stated in [11–13], causal effect modeling, visualized in Figure 2, is helpful for a machine learning task, e.g., image/frame classification, and affects model performance in a positive way. In this work, a new causal video summarizer (CVS) is proposed that tackles the aforementioned issue to improve the performance of a multi-modal video summarization model. The proposed causality-based model consists of a multi-modal feature processing module (MFPM), probabilistic encoding module (PEM), and a probabilistic decoding module (PDM), referring to Figure 3. Studying multi-modal video summarization from the causality perspective [11] eliminates the need for a priori definition of objectives [9] based on high-level concepts. For the implicit interaction between the video and query, an attention mechanism is applied to better capture the interactive information.

According to [14], typically the generated video summary by a video summarization algorithm is composed of a set of representative video frames or video fragments. Frame-based video summaries are not restricted by timing or synchronization issues and, therefore, they provide more flexibility in terms of data organization for video exploration purpose [14, 15]. In this work, the proposed CVS is validated on the frame-based multi-modal video summarization dataset

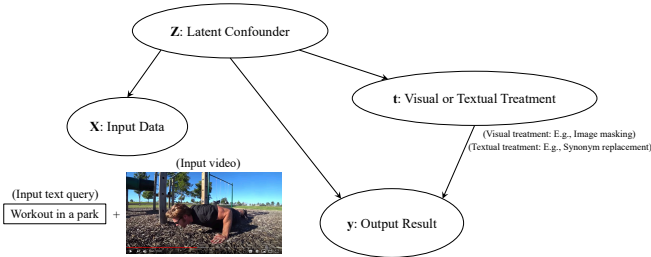


Fig. 2: Explanation of the causal effect modeling concept, i.e., causal graphical model [11], in multi-modal video summarization. \mathbf{t} is a treatment, e.g., visual or textual perturbation [12]. \mathbf{y} is an outcome, e.g., an importance score of a video frame or a relevance score between the input text-based query and video. \mathbf{Z} is an unobserved confounder, e.g., representativeness or interestingness [4, 9, 16]. \mathbf{X} is a noisy view [11] on the hidden confounder \mathbf{Z} , say the input text query and video.

[10]. Experimental results show that the proposed method is effective and significantly increases both the accuracy and $F1$ -score, compared with the state-of-the-art method.

2. RELATED WORK

2.1 Video Summarization with A Single Modality

Recently, a number of methods with different techniques have been proposed for video summarization, such as [1, 3, 4, 16, 17]. In [4, 16], human-explainable concepts, e.g., interestingness and representativeness, are used to characterize a good video summary. Then, objectives are built based on those concepts. Visual and textual information related to a video can then be captured by the targeted objectives. However, a notable limitation is that it is hard to define/measure all possible confounders [11] a priori, such as compactness [17], uniformity, and representativeness [4]. In [1, 17], an attention mechanism, a generative adversarial network, and reinforcement learning are used to perform video summarization. Since video summarization with a single modality cannot effectively help video exploration [9, 10], in this work a new multi-modal video summarization model is proposed to address this problem.

2.2 Multi-modal Video Summarization

Instead of only considering the visual input, several works have investigated the potential of using additional modalities, e.g., viewers’ comments, video captions, or any other available contextual data, to help models’ performance. [9, 10, 18–36]. In [25], a multi-modal video summarization method is introduced for key-frame extraction from first-person videos. In [18], a multi-modal deep-learning-based model is proposed to summarize videos of soccer games. In [19], a semantic-based video fragment selection and a visual-to-text mapping are applied based on the relevance between the original and the automatically-generated video descriptions, with the help of semantic attended networks. Existing multi-modal video summarization models do not focus on causal effect modeling [11]. Hence, the interactive information between the video and query is difficult to capture effectively. In this work, a new causality-based multi-modal video summarization method is introduced, based on a probabilistic encoder-decoder framework and attention mechanism, to better capture the interaction between the video and query and make

the video exploration more effective.

2.3 Causality and Variational Autoencoders

Proxy variables, e.g., input data \mathbf{X} in Figure 2, and the challenges about how to use them correctly have been considered in the literature of causal inference [37]. In many observational studies [4, 16, 38], understanding the best way to derive and measure possible proxy variables is crucial. Building on the previous work [39, 40], the authors of [11] and recent works [38, 41] for vision applications have tried to exploit proxy variables to study conditions for causal identifiability. In many cases, the general idea is that one should first attempt to infer the joint distribution $p(\mathbf{X}, \mathbf{Z})$ between the hidden confounders and the proxy, and then use that knowledge to adjust for the hidden confounders [42–44]. Take the causal graphical model in Figure 2 as an example. The authors of [43] have shown that if \mathbf{X} and \mathbf{Z} are categorical, with \mathbf{X} having at least as many categories as \mathbf{Z} , and with the matrix $p(\mathbf{X}, \mathbf{Z})$ being full-rank, one could use a matrix inversion formula, an approach called “effect restoration” [44], to identify the causal effect of \mathbf{t} on \mathbf{y} , referring to *Methodology* section for details. Recently, the authors of [42] have given the conditions under which one could identify more complicated and general proxy models. The proposed causality-based method for multi-modal video summarization is mainly inspired by [11, 37, 43, 45].

3. METHODOLOGY

3.1 Causal Video Summarizer (CVS)

In this section, details of the proposed CVS are described. Note that causal effect modeling for real-world multi-modal video summarization is very complicated [11]. Hence, in this work, the assumptions mentioned in [11] are followed to model the problem of multi-modal video summarization based on the concept of causal effect inference, i.e., causal graphical model. The proposed CVS is mainly composed of a multi-modal feature processing module (MFPM), a probabilistic encoding module (PEM), and a probabilistic decoding module (PDM), referring to Figure 3. The generation of a good video summary is affected by latent factors. In this work, the latent factors are considered as the causal effect. Specifically, the concept of causal effect inference [11], i.e., a causal graphical model, is used to model the multi-modal video summarization problem, referring to Figure 2. Figure 2 contains the four key components of the causal graphical model: “input data (\mathbf{X})”, “latent confounder (\mathbf{Z})”, “treatment (\mathbf{t})”, and “output result (\mathbf{y})”. From the modeling perspective of multi-modal video summarization, \mathbf{X} is “an input video with a text query”. \mathbf{t} is “a visual or textual treatment”. Note that treatment in causal effect modeling is a way to make an input characteristic more salient and help a model learn better [11]. \mathbf{y} is “a relevance score between the input text-based query and video frame or an importance score of a video frame”. \mathbf{Z} is “a variational latent representation” which the proposed model aims to learn from \mathbf{X} for reconstruction [11, 45], referring to Figure 3 for the practical implementation. The proposed causal model simultaneously generates outcome score labels \mathbf{y} when \mathbf{X} is reconstructed, illustrated in Figure 3. Thereafter, video summaries can be created based on the generated outcome score labels.

Objective function for training. According to [11, 45, 46], variational autoencoder (VAE) aims to learn a variational la-

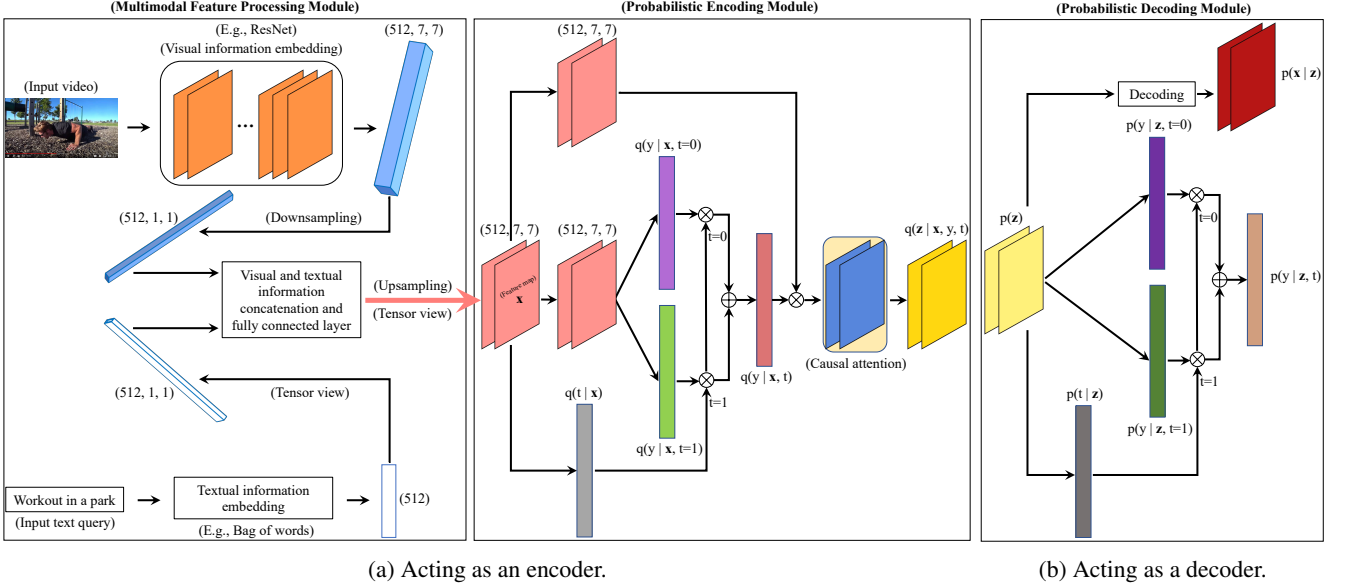


Fig. 3: This figure shows the proposed end-to-end causal attention model for multi-modal video summarization, the practical implementation of the causal graphical model in Figure 2. In (a), the input video and input text query are processed by MFPM for generating the feature map \mathbf{x} which is the input of PEM. Then, PEM generates the corresponding probabilistic encoding $q(\mathbf{z}|\mathbf{x}, y, t)$ of \mathbf{x} with the operations of the introduced causal attention. In (b), PDM takes $p(\mathbf{z})$, estimated by $q(\mathbf{z}|\mathbf{x}, y, t)$, to approximately reconstruct \mathbf{x} based on $p(\mathbf{x}|\mathbf{z})$ and generate the prediction score labels y based on $p(y|\mathbf{z}, t)$ at the same time. Please refer to *Methodology* section for details.

tent representation \mathbf{Z} from data \mathbf{X} for reconstruction; it is capable of learning the latent variables when used in a causal graphical model. Hence, the proposed CVS is built on top of VAE. Now, it is time to form a single objective for the encoder, in Figure 3-(a), and the decoder, in Figure 3-(b), to learn meaningful causal representations in the latent space and generate video summaries. Based on Figure 2, we know that the true posterior over \mathbf{Z} depends on not just \mathbf{X} , but also on \mathbf{t} and \mathbf{y} . We have to know the treatment assignment \mathbf{t} along with its outcome \mathbf{y} before inferring the distribution over \mathbf{Z} . Hence, the following two auxiliary distributions are introduced for the treatment assignment \mathbf{t} and the outcome \mathbf{y} , referring to Equations (1), and (2).

$$q(t_i|\mathbf{x}_i) = \text{Bern}(\sigma(g_{\phi_5}(\mathbf{x}_i))) \quad (1)$$

$$q(y_i|\mathbf{x}_i, t_i) = \sigma(t_i g_{\phi_6}(\mathbf{x}_i) + (1 - t_i) g_{\phi_7}(\mathbf{x}_i)), \quad (2)$$

where $g_{\phi_k}(\cdot)$ is a neural network with variational parameters ϕ_k for $k = 5, 6, 7$. Note that, unlike traditional VAEs simply passing the feature map directly to the latent space, i.e., the upper path of PEM in Figure 3-(a), the feature map is also sent to the other two paths, i.e., the middle and the lower paths in PEM in Figure 3-(a), for the posterior estimations of the treatment t_i and the outcome y_i .

The introduced auxiliary distributions help us predict t_i and y_i for new samples. To estimate the parameters of these two distributions, $q(t_i|\mathbf{x}_i)$ and $q(y_i|\mathbf{x}_i, t_i)$, we add an auxiliary objective, referring to Equation (3), to the model training objective over N data samples.

$$\mathcal{L}_{auxiliary} = \sum_{i=1}^N (\log q(t_i = t_i^*|\mathbf{x}_i^*) + \log q(y_i = y_i^*|\mathbf{x}_i^*, t_i^*)), \quad (3)$$

where \mathbf{x}_i^* , t_i^* and y_i^* are observed values in the training set.

Finally, we have the following overall training objective for the encoder and decoder networks. See Equation (4).

$$\mathcal{L}_{causal} = \mathcal{L}_{auxiliary} +$$

$$\sum_{i=1}^N \mathbb{E}_{q(\mathbf{z}_i|\mathbf{x}_i, t_i, y_i)} [\log p(\mathbf{x}_i, t_i|\mathbf{z}_i) + \log p(y_i|t_i, \mathbf{z}_i) + \log p(\mathbf{z}_i) - \log q(\mathbf{z}_i|\mathbf{x}_i, t_i, y_i)]. \quad (4)$$

See [11] for the detailed derivation and explanation of Equations (1) to (4), $\log p(\mathbf{x}_i, t_i|\mathbf{z}_i)$, $\log p(y_i|t_i, \mathbf{z}_i)$, and $\log p(\mathbf{z}_i)$.

3.2 Spatial and Channel-wise Attentions

A dual attention network, based on self-attention, has been proposed to adaptively integrate local features with their global dependencies [47,48]. The dual attention network consists of spatial and channel-wise attention modules. These two modules are capable of modeling the interdependencies in spatial and channel dimensions. To better capture the implicit interactive information, a causal attention mechanism, based on the dual attention network, is introduced to reinforce the probabilistic encoder in Figure 3-(a). In the PEM, the channel-wise attention selectively emphasizes interdependent channel maps by integrating associated features among all channel maps. The spatial attention selectively aggregates the feature at each position by a weighted sum of the features at all positions.

3.3 Video Summary Generation

In Figure 3-(a), during the inference phase, the input video and input text-based query go through the MFPM for generating feature maps \mathbf{x} , and the PEM for generating the probabilistic encoding of the feature maps $q(\mathbf{z}|\mathbf{x}, y, t)$. Then, the generated probabilistic encoding of the feature maps is sent

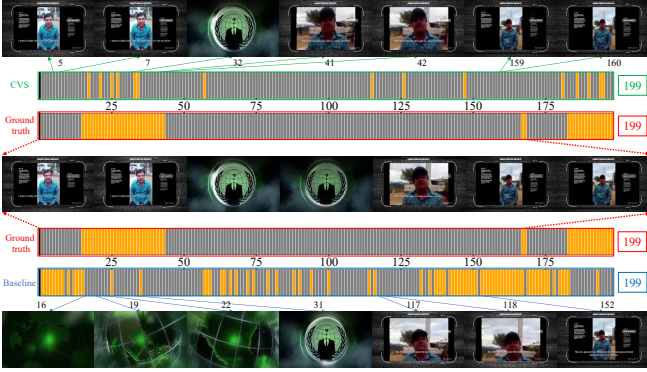


Fig. 4: This figure shows the randomly selected qualitative results of the proposed causal model and the baseline model. According to this figure, we see that the proposed model (in green) prediction result frame pattern is more similar to the ground truth (in red) pattern than the baseline (in blue). Note that in each frame pattern, orange denotes “not selected frames” and gray denotes “selected frames”. Each video here has 199 frames and we also show the corresponding indices of the selected frames in this figure.

to the probabilistic decoder, referring to Figure 3-(b), to reconstruct \mathbf{x} , based on $p(\mathbf{x}|\mathbf{z})$, and generate prediction score labels y , based on $p(y|\mathbf{z}, t)$, for the input video and query simultaneously. Finally, based on these generated score labels, a set of video frames is selected from the original input video to create the final video summary. Note that the video summary budget is considered as a user-defined hyperparameter in video exploration [10].

4. EXPERIMENTS

4.1 Dataset and Evaluation Metrics

In the experiments, [10]’s multi-modal video summarization dataset and the introduced causal video summarization dataset (CVSD) with treatment labels are used to verify the proposed method. The introduced CVSD is constructed based on [10]’s dataset. [10]’s dataset is composed of 190 videos with a duration of two to three minutes for each video. Each video in their dataset is retrieved based on a given text-based query. The entire dataset is divided into splits of 60%/20%/20% for training/validation/testing, respectively. Annotations from human experts are necessary for the automatic evaluation of multi-modal video summarization. Hence, the authors of [10] sample all of the 190 videos at one frame per second (fps), and Amazon Mechanical Turk (AMT) is used to annotate every frame with its relevance score with respect to the given text-based query. A single ground truth relevance score is created for each query-video pair by merging the corresponding relevance annotations from AMT workers. In [10]’s dataset, the maximum number of words of a text query is 8 and the maximum number of frames of video is 199.

For the evaluation metric, the authors of [10] propose to use accuracy as the evaluation metric. That is, a predicted relevance score is considered correct when the predicted score is the same as the majority of human experts’ provided score. In addition, motivated by [3,49], in this work F_1 -score is also

used to quantify the performance of the proposed model by measuring the agreement between the gold standard and predicted scores provided by the human experts.

4.2 Experimental Setup

In this work, [10]’s dataset and the introduced CVSD have the same preprocessing as follows. Since the video lengths in the CVSD and [10]’s dataset are varied, the number of frames for each video is different based on $\text{fps} = 1$. The maximum number of frames of a video is 199 in the used dataset. Hence, the frame-repeating video preprocessing technique [10] is adopted to make all the videos have the same length of 199. ResNet [50] pre-trained on ImageNet [51] is used to extract 199 frame-based features for each video, and the feature used is located in the visual layer one layer below the classification layer. The input frame size of the ResNet is 224 by 224 with red, green, and blue channels. Each image channel is normalized by mean = (0.4280, 0.4106, 0.3589) and standard deviation = (0.2737, 0.2631, 0.2601). PyTorch is used for the implementation and to train models with 50 epochs, 0.01 learning rate, and Adam optimizer [52]. For the hyperparameters of the Adam, $\beta_1 = 0.9$ and $\beta_2 = 0.999$ are the coefficients used for computing moving averages of gradient and its square. The term added to the denominator to improve numerical stability is $\epsilon = 10^{-8}$.

4.3 Effectiveness Analysis

Effectiveness of Causal Attention Mechanism. In the experiments, the CVSD is used to verify the effectiveness of the introduced attention mechanism under the following six different situations of inputs: “visual input with salt and pepper treatment ($V_{s\&p}$)”, “visual input with blurring treatment (V_{blur})”, “clean text-based query input and visual input with salt and pepper treatment ($T + V_{s\&p}$)”, “clean text-based query input and visual input with blurring treatment ($T + V_{blur}$)”, “disturbed text-based query input and visual input with salt and pepper treatment ($T_k + V_{s\&p}$)”, and “disturbed text-based query input and visual input with blurring treatment ($T_k + V_{blur}$)”. Note that T_k denotes randomly removing k words, e.g., $k = 2$, from a text-based query input. According to Table 1, the results show that the introduced attention mechanism results in performance improvement in the causal model. The main reason is that the introduced attention mechanism helps to better capture the implicit interactive information between the visual and textual inputs.

Effectiveness of Causal Effect Modeling. The main difference between the proposed causal model and the existing state-of-the-art multi-modal video summarization method, e.g., [10], is the causal effect modeling. According to [11], proper causal effect modeling improves the performance of a machine learning model. In this work, we claim that if the causal effect modeling is effective, the proposed model’s performance can be improved. Based on Table 1 and Table 2, the results show that the proposed causal model for multi-modal video summarization beats the state-of-the-art [10], with the increase of +5.4% in accuracy and +4.92% increase of F_1 -score. The main reason is the proposed model is a causality-based model which properly considers the causal effect modeling. Hence, the claim is well proved by the experimental results. Qualitative results are presented in Figure 4.

Table 1: Ablation study of the introduced attention mechanism and comparison with the state-of-the-art multi-modal video summarization model “QueryVS” [10]. The results are based on the introduced CVSD and the metric of accuracy from [10]. The attention mechanism is effective and the proposed CVS outperforms the “QueryVS” model in the metric of accuracy under six different situations of inputs. Please refer to the *Effectiveness Analysis* section for the definitions of notations in the table.

Model	$V_{s\&p}$	V_{blur}	$T + V_{s\&p}$	$T + V_{blur}$	$T_k + V_{s\&p}$	$T_k + V_{blur}$
QueryVS [10]	0.629	0.507	0.547	0.533	0.501	0.488
CVS with attention	0.687	0.596	0.554	0.535	0.532	0.524
CVS without attention	0.676	0.423	0.442	0.530	0.514	0.500

Table 2: Comparison with the state-of-the-art model “QueryVS” [10] validated on [10]’s dataset. The results are based on the metric of accuracy [10] and F_1 -score [49]. Proposed CVS outperforms the model in [10] by +5.4% in accuracy and +4.92% in F_1 -score.

Evaluation Metric	Accuracy	F_1 -score
QueryVS [10]	0.704	0.508
CVS	0.742	0.533

5. CONCLUSION

In this work, a new perspective is introduced to build an end-to-end deep causal model for multi-modal video summarization. The proposed Causal Video Summarizer is based on a probabilistic encoder-decoder architecture. Experimental results show that the proposed causal model is effective and achieves state-of-the-art performance, +5.4% in accuracy and +4.92% increase of F_1 -score.

6. ACKNOWLEDGMENTS

This project has received funding from the European Union’s Horizon 2020 research and innovation programme under the Marie Skłodowska-Curie grant agreement No 765140.

7. REFERENCES

- [1] Zhong Ji, Kailin Xiong, Yanwei Pang, and Xuelong Li, “Video summarization with attention-based encoder-decoder networks,” *IEEE Transactions on Circuits and Systems for Video Technology*, 2019.
- [2] Danila Potapov, Matthijs Douze, Zaid Harchaoui, and Cordelia Schmid, “Category-specific video summarization,” in *ECCV*, 2014, pp. 540–555.
- [3] Yale Song, Jordi Vallmitjana, Amanda Stent, and Alejandro Jaimes, “Tvsum: Summarizing web videos using titles,” in *Conference on Computer Vision and Pattern Recognition*, 2015, pp. 5179–5187.
- [4] Michael Gygli, Helmut Grabner, and Luc Van Gool, “Video summarization by learning submodular mixtures of objectives,” in *Conference on Computer Vision and Pattern Recognition*, 2015, pp. 3090–3098.
- [5] Ke Zhang, Wei-Lun Chao, Fei Sha, and Kristen Grauman, “Summary transfer: Exemplar-based subset selection for video summarization,” in *Proceedings of the IEEE conference on computer vision and pattern recognition*, 2016, pp. 1059–1067.
- [6] Yujia Zhang, Michael Kampffmeyer, Xiaoguang Zhao, and Min Tan, “Dtr-gan: Dilated temporal relational adversarial network for video summarization,” in *Proceedings of the ACM Turing Celebration Conference-China*, 2019, pp. 1–6.
- [7] Sandra Eliza Fontes De Avila, Ana Paula Brandão Lopes, Antonio da Luz Jr, and Arnaldo de Albuquerque Araújo, “Vsumm: A mechanism designed to produce static video summaries and a novel evaluation method,” *Pattern Recognition Letters*, vol. 32, no. 1, pp. 56–68, 2011.
- [8] Aidean Sharghi, Ali Borji, Chengtao Li, Tianbao Yang, and Boqing Gong, “Improving sequential determinantal point processes for supervised video summarization,” in *European Conference on Computer Vision*, 2018, pp. 517–533.
- [9] Arun Balajee Vasudevan, Michael Gygli, Anna Volokitin, and Luc Van Gool, “Query-adaptive video summarization via quality-aware relevance estimation,” in *Proceedings ACM MM*, 2017, pp. 582–590.
- [10] Jia-Hong Huang and Marcel Worring, “Query-controllable video summarization,” in *ICMR*, 2020, pp. 242–250.
- [11] Christos Louizos, Uri Shalit, Joris M Mooij, David Sonntag, Richard Zemel, and Max Welling, “Causal effect inference with deep latent-variable models,” in *NIPS*, 2017, pp. 6446–6456.
- [12] Chao-Han Huck Yang, I Hung, Te Danny, Yi Ouyang, and Pin-Yu Chen, “Training a resilient q-network against observational interference,” *AAAI*, 2022.
- [13] Chao-Han Huck Yang, I Hung, Te Danny, Yi-Chieh Liu, and Pin-Yu Chen, “Treatment learning transformer for noisy image classification,” *arXiv preprint arXiv:2203.15529*, 2022.
- [14] Evlampios Apostolidis, Eleni Adamantidou, Alexandros I Metsai, Vasileios Mezaris, and Ioannis Patras, “Video summarization using deep neural networks: A survey,” *arXiv preprint arXiv:2101.06072*, 2021.
- [15] Janko Calic, David P Gibson, and Neill W Campbell, “Efficient layout of comic-like video summaries,” *IEEE Transactions on Circuits and Systems for Video Technology*, vol. 17, no. 7, pp. 931–936, 2007.
- [16] Bryan A Plummer, Matthew Brown, and Svetlana Lazebnik, “Enhancing video summarization via vision-language embedding,” in *Conference on Computer Vision and Pattern Recognition*, 2017, pp. 5781–5789.
- [17] Yujia Zhang, Michael Kampffmeyer, Xiaodan Liang, Dingwen Zhang, Min Tan, and Eric P Xing, “Dilated temporal relational adversarial network for generic video summarization,” *Multimedia Tools and Applications*, vol. 78, no. 24, pp. 35237–35261, 2019.
- [18] Melissa Sanabria, Frédéric Precioso, and Thomas Mengy, “A deep architecture for multimodal summarization of soccer games,” in *International Workshop on Multimedia Content Analysis in Sports*, 2019, pp. 16–24.

- [19] Huawei Wei, Bingbing Ni, Yichao Yan, Huanyu Yu, Xiaokang Yang, and Chen Yao, "Video summarization via semantic attended networks," in *AAAI*, 2018, vol. 32.
- [20] Jia-Hong Huang, Luka Murn, Marta Mrak, and Marcel Worring, "Gpt2mvs: Generative pre-trained transformer-2 for multi-modal video summarization," in *ICMR*, 2021, pp. 580–589.
- [21] Jia-Hong Huang, Modar Alfadly, Bernard Ghanem, and Marcel Worring, "Assessing the robustness of visual question answering," *arXiv:1912.01452*, 2019.
- [22] Jia-Hong Huang, Cuong Duc Dao, Modar Alfadly, and Bernard Ghanem, "A novel framework for robustness analysis of visual qa models," in *AAAI*, 2019, vol. 33, pp. 8449–8456.
- [23] Jia-Hong Huang, Modar Alfadly, and Bernard Ghanem, "Vqabq: Visual question answering by basic questions," *VQA Challenge Workshop, CVPR*, 2017.
- [24] Tao Hu, Pascal Mettes, Jia-Hong Huang, and Cees GM Snoek, "Silco: Show a few images, localize the common object," in *ICCV*, 2019, pp. 5067–5076.
- [25] Yujie Li, Atsunori Kanemura, Hideki Asoh, Taiki Miyanishi, and Motoaki Kawanabe, "Extracting key frames from first-person videos in the common space of multiple sensors," in *ICIP. IEEE*, 2017, pp. 3993–3997.
- [26] Jia-Hong Huang, Modar Alfadly, and Bernard Ghanem, "Robustness analysis of visual qa models by basic questions," *VQA Challenge and Visual Dialog Workshop, CVPR*, 2018.
- [27] Jia-Hong Huang, Ting-Wei Wu, and Marcel Worring, "Contextualized keyword representations for multi-modal retinal image captioning," in *ICMR*, 2021, pp. 645–652.
- [28] Jia-Hong Huang, Ting-Wei Wu, Chao-Han Huck Yang, and Marcel Worring, "Deep context-encoding network for retinal image captioning," in *ICIP. IEEE*, 2021, pp. 3762–3766.
- [29] Jia-Hong Huang, Ting-Wei Wu, Chao-Han Huck Yang, and Marcel Worring, "Longer version for" deep context-encoding network for retinal image captioning," *arXiv preprint arXiv:2105.14538*, 2021.
- [30] C-H Huck Yang, Fangyu Liu, Jia-Hong Huang, Meng Tian, I-Hung Lin, Yi Chieh Liu, Hiromasa Morikawa, Hao-Hsiang Yang, and Jesper Tegner, "Auto-classification of retinal diseases in the limit of sparse data using a two-streams machine learning model," in *ACCV*. Springer, 2018, pp. 323–338.
- [31] Yi-Chieh Liu, Hao-Hsiang Yang, C-H Huck Yang, Jia-Hong Huang, Meng Tian, Hiromasa Morikawa, Yi-Chang James Tsai, and Jesper Tegner, "Synthesizing new retinal symptom images by multiple generative models," in *ACCV*. Springer, 2018, pp. 235–250.
- [32] C-H Huck Yang, Jia-Hong Huang, Fangyu Liu, Fang-Yi Chiu, Mengya Gao, Weifeng Lyu, Jesper Tegner, et al., "A novel hybrid machine learning model for auto-classification of retinal diseases," *Workshop on Computational Biology, ICML*, 2018.
- [33] Riccardo Di Sipio, Jia-Hong Huang, Samuel Yen-Chi Chen, Stefano Mangini, and Marcel Worring, "The dawn of quantum natural language processing," *ICASSP*, 2022.
- [34] Jia-Hong Huang, "Robustness analysis of visual question answering models by basic questions," *King Abdulah University of Science and Technology, Master Thesis*, 2017.
- [35] Jia-Hong Huang, C-H Huck Yang, Fangyu Liu, Meng Tian, Yi-Chieh Liu, Ting-Wei Wu, I Lin, Kang Wang, Hiromasa Morikawa, Hernghua Chang, et al., "Deepopht: medical report generation for retinal images via deep models and visual explanation," in *WACV*, 2021, pp. 2442–2452.
- [36] Jia-Hong Huang, Ting-Wei Wu, C-H Huck Yang, Zenglin Shi, I Lin, Jesper Tegner, Marcel Worring, et al., "Non-local attention improves description generation for retinal images," in *WACV*, 2022, pp. 1606–1615.
- [37] Peter A Frost, "Proxy variables and specification bias," *The review of economics and Statistics*, p. 323, 1979.
- [38] Dong Zhang, Hanwang Zhang, Jinhui Tang, Xiansheng Hua, and Qianru Sun, "Causal intervention for weakly-supervised semantic segmentation," *NIPS*, 2020.
- [39] Sander Greenland and DAVID G KLEINBAUM, "Correcting for misclassification in two-way tables and matched-pair studies," *International Journal of Epidemiology*, vol. 12, no. 1, pp. 93–97, 1983.
- [40] Jan Selén, "Adjusting for errors in classification and measurement in the analysis of partly and purely categorical data," *Journal of the American Statistical Association*, vol. 81, no. 393, pp. 75–81, 1986.
- [41] Ehsan Abbasnejad, Damien Teney, Amin Parvaneh, Javen Shi, and Anton van den Hengel, "Counterfactual vision and language learning," in *CVPR*, 2020, pp. 10044–10054.
- [42] Wang Miao, Zhi Geng, and Eric J Tchetgen Tchetgen, "Identifying causal effects with proxy variables of an unmeasured confounder," *Biometrika*, vol. 105, no. 4, pp. 987–993, 2018.
- [43] Judea Pearl, "On measurement bias in causal inference," *arXiv preprint arXiv:1203.3504*, 2012.
- [44] Manabu Kuroki and Judea Pearl, "Measurement bias and effect restoration in causal inference," *Biometrika*, vol. 101, no. 2, pp. 423–437, 2014.
- [45] Diederik P Kingma and Max Welling, "Auto-encoding variational bayes," *arXiv:1312.6114*, 2013.
- [46] Uri Shalit, Fredrik D Johansson, and David Sontag, "Estimating individual treatment effect: generalization bounds and algorithms," in *ICML*, 2017, p. 3076.
- [47] Jun Fu, Jing Liu, Haijie Tian, Yong Li, Yongjun Bao, Zhiwei Fang, and Hanqing Lu, "Dual attention network for scene segmentation," in *CVPR*, 2019, p. 3146.
- [48] Ashish Vaswani, Noam Shazeer, Niki Parmar, Jakob Uszkoreit, Llion Jones, Aidan N Gomez, Lukasz Kaiser, and Illia Polosukhin, "Attention is all you need," *arXiv preprint arXiv:1706.03762*, 2017.
- [49] George Hripcsak and Adam S Rothschild, "Agreement, the f-measure, and reliability in information retrieval," *Journal of the American medical informatics association*, vol. 12, no. 3, pp. 296–298, 2005.
- [50] Kaiming He, Xiangyu Zhang, Shaoqing Ren, and Jian Sun, "Deep residual learning for image recognition," in *CVPR*, 2016, pp. 770–778.
- [51] Jia Deng, Wei Dong, Richard Socher, Li-Jia Li, Kai Li, and Li Fei-Fei, "Imagenet: A large-scale hierarchical image database," in *CVPR. IEEE*, 2009, pp. 248–255.
- [52] Diederik P Kingma and Jimmy Ba, "Adam: A method for stochastic optimization," *arXiv:1412.6980*, 2014.